Effects of Solute−Solvent Proton Exchange on Polypeptide Chain Dynamics: A Constant-pH Molecular Dynamics Study

M. Długosz and J. M. Antosiewicz*

Department of Biophysics, Warsaw University, Żwirki i Wigury 93, Warsaw 02-089, Poland

Received: February 2, 2005; In Final Form: April 7, 2005

A method for performing implicit-solvent molecular dynamics simulations at constant pH was applied to a pentapeptide acetyl-Ala-Asp-Ala-Lys-Ala-amide at pH 4. As a reference, molecular dynamics simulations were done for the same peptide with two variants of its fixed protonation patterns expected to dominate at pH 4, i.e., with a protonated and a deprotonated side chain of the Asp residue and the protonated Lys residue in both cases. The dynamic trajectories of the peptide were used to discuss the problem of the significance of the solute−solvent proton exchange phenomena for the dynamics and structural distributions of the polypeptide chain. The Asp−Lys distance was used as a probe of the overall molecular structure of the investigated pentapeptide. To characterize the dynamics, distributions of the "waiting" times for a transition from a "short" distance conformation to a "long" distance conformation were constructed, based on the generated molecular dynamics trajectories. We show that the relaxation time for the transitions, derived from the constant-pH simulations, is very close to the relaxation time characterizing a permanently protonated molecule, although the average protonation probability of the short-distance conformation is close to zero. However, the distribution of the Asp−Lys distances obtained from constant-pH simulations cannot be reproduced as a linear combination of the distributions resulting from the simulations with fixed protonation states.

Introduction

Polypeptides and proteins usually have a number of ionizable side chains that can release or bind protons to become negatively or positively charged.[1] Because of the long-range nature of electrostatic interactions, these proton exchange phenomena are expected to have a substantial impact on the molecular structure, dynamics, and other physicochemical properties. Experimental and theoretical studies of the coupling between protein conformation and ionization equilibria usually consider pH effects on different molecular properties such as structural stability,[2−7] induction of conformational changes,[8−10] and structural consequences of mutating titratable residues into nontitratable ones[11] or their neutralization.[12] An interesting question, which cannot be answered directly by an observation of the consequences of a change in the solution pH or mutations of titratable residues, is related to the impact of the existence of a microscopic degree of freedom, resulting from the proton exchange phenomena, on the dynamics and structural preferences of molecules possessing titratable groups. It seems that a computer simulation method, called constant-pH molecular dynamics, constitutes a valuable tool to study this problem.

Molecular dynamics (MD) is a well-established theoretical method for studying properties of molecules;[13] however, the problem of protonation equilibria was usually treated in a simplified way so far: Titratable residues were assigned fixed protonation states expected for their type and solution pH. A number of existing quantum-mechanical simulation methods that allow the protonation states of ionizable groups to change in time represent the most realistic approach available to describe proton exchange phenomena. These include quantum-mechanical dynamics,[14] hybrid quantum−classical dynamics,[15−17] and classical dynamics using fitted potentials.[17,18] These simulation algorithms are computationally too expensive to be suitable for the generation of sufficiently long dynamic trajectories of (bio)-molecules possessing a number of titratable groups. Hence, less accurate models, including constant-pH molecular dynamics methods, are developed and used.

Constant-pH molecular dynamics algorithms have been introduced, during the past decade, by several groups, some of them using an implicit[19−22] and others using an explicit description of the proton exchange processes.[23−28] Implicit proton exchange algorithms employ protonation parameters that allow the protonation state for each titration site to vary continuously. Consequently, the various protonation states are not sampled, but the protonation fraction, assigned to each residue, is adjusted appropriately to the electrostatic potential at the ionizable site. The explicit proton exchange algorithm developed by Baptista et al.[24] uses the Poisson−Boltzmann equation to calculate the protonation energies used in Monte Carlo sampling to select protonation states and explicit solvent Newtonian dynamics between the selection steps. The explicit protonation algorithm of Mongan et al.[28] uses generalized Born electrostatics for calculating transition energies between protonation states and for describing solvation effects during molecular dynamics. Finally, the algorithm of Bürgi and coworkers[23] is an explicit solvent algorithm that generates trajectories at a Boltzmann-distributed ensemble of protonation states by a combination of molecular dynamics and Monte Carlo simulation. At each Monte Carlo step of their algorithm, an explicit change in the protonation state of a titratable residue is attempted, and the free energy difference of the change is calculated with the thermodynamic integration method, followed

* Author to whom correspondence should be addressed. E-mail: jantosi@biogeo.uw.edu.pl.

10.1021/jp0505779 CCC: $30.25
Published on Web 06/24/2005

by the usual Monte Carlo procedure for acceptance or rejection of the attempted protonation state.

A qualitative agreement between predicted and experimental pK_a values, obtained by these algorithms, indicates that they reasonably accurately sample the protonation and conformation states of investigated systems and that they can be used to study pH-dependent phenomena in proteins and other molecules. Börjesson and Hünenberger described an application of their implicit proton exchange constant-pH molecular dynamics algorithm to investigate the stability of a decalysine α-helix.[22] Mongan et al.[28] applied their explicit protonation and implicit-solvent-treatment algorithm in the investigation of the coupling of conformation and protonation in hen egg-white lysozyme.

We present here a discussion of the significance of the proton exchange phenomena for acetyl-Ala-Asp-Ala-Lys-Ala-amide polypeptide chain dynamics and conformation. We compare results of constant-pH molecular dynamics simulations at single value of solvent pH, with corresponding results obtained from molecular dynamics simulations with fixed protonation states of the titratable residues. Our results clearly indicate that the protonation equilibria affect both conformational relaxation times and distributions of adopted conformations in a way that cannot be predicted by referring to the results of simulations performed with fixed protonation states of the titratable residues.

Models and Methods

Description of Structural Properties of the Acetyl-Ala-Asp-Ala-Lys-Ala-Amide Pentapeptide. As a test molecule for the investigations described in this work, we used a pentapeptide acetyl-Ala-Asp-Ala-Lys-Ala-amide. This choice was dictated by the results of our previous studies,[26,36] investigating pH-dependent structural properties of a heptapeptide, acetyl-Ser-Asp-Asn-Lys-Thr-Tyr-Gly-amide, derived from ovomucoid third domain (OMTKY3). In the most recent study,[36] we analyzed two overall molecular characteristics of this heptapeptide (distributions of protonation fractions of Asp2 side chain and distributions of Asp−Lys distances), and we showed that these characteristics, when obtained from constant-pH molecular dynamics simulations, cannot be reproduced by linear combinations of the characteristics obtained from fixed protonation state simulations. The main purpose of the present study is to extend this kind of investigation into the conformational dynamics domain. Analysis of this problem using the heptapeptide as a test molecule or one of a peptide for which NMR data regarding molecular conformation as a function of pH exist, which are even longer, would require much longer molecular dynamics trajectories. Thus, for the current study we decided to choose a much simpler system. The choice of the pentapeptide acetyl-Ala-Asp-Ala-Lys-Ala-amide is justified by three important reasons: (1) Its behavior, related to the proton exchange phenomena, is expected to be dominated by two centers located on its two titratable residues without any significant disturbing influence from the remaining parts of the chain. (2) The pK_a values of the Asp and Lys side chains are well-separated and not expected to be significantly changed by conformational changes, and therefore simulations at pH 4 need to take into account only the protonation equilibria of the Asp residue. (3) It is sufficiently small, so many long molecular dynamics trajectories can be simulated using PC work stations at an acceptable CPU time expense.

A model of the acetyl-Ala-Asp-Ala-Lys-Ala-amide pentapeptide is shown in Figure 1. To describe the overall structural properties of this molecule, we measured the distance between the CG atom of the Asp2 residue and the N-atom of the Lys4 residue (atom names are taken as they appear in the Protein Data Bank structural files). We made such a choice mainly because of the expectation that the electrostatic interaction between the negatively charged in its ionized state Asp side chain and the permanently positively charged (at the pH of the simulations) Lys should influence this distance. Strong correlation between the measured Asp−Lys distance and the average protonation of the pentapeptide shown in Figure 6 confirm the appropriateness of our choice.

On the basis of the structures sampled from the ensembles of simulated molecular dynamics trajectories, with both fixed and variable protonation states of the Asp2 side chain of the pentapeptide, we collected distances between the CG atom of the Asp2 residue and the N-atom of the Lys4 residue, the duration of "short" and "long" Asp−Lys distance structures, and the protonation fractions of the Asp2 residue side chain. Figure 2 shows examples of pentapeptides corresponding to the short and long Asp−Lys distance conformers.

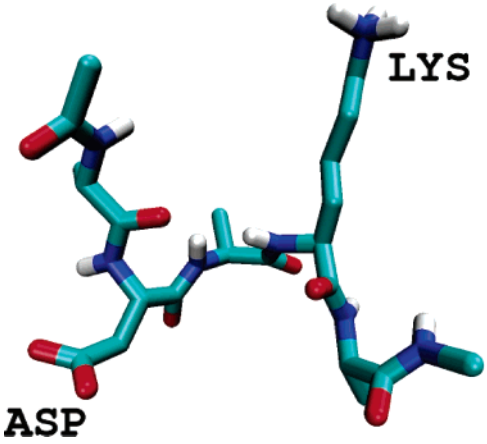

Figure 1. Structure of the acetyl-Ala-Asp-Ala-Lys-Ala-amide pentapeptide in the heavy atom representation.

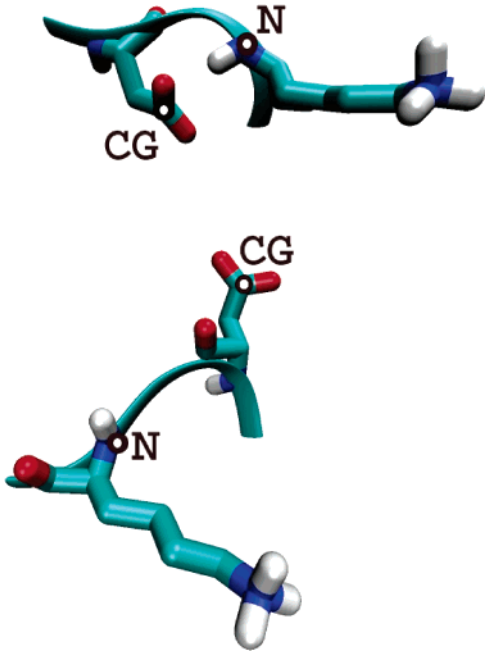

Figure 2. Representative structures of the pentapeptide acetyl-Ala-Asp-Ala-Lys-Ala-amide. Top panel: A short Asp−Lys distance conformer. Bottom panel: A long Asp−Lys distance conformer. White spots indicate the N-atom of the Lys residue and the CG atom of the Asp residue defining the distance between those residues.

Constant-pH Molecular Dynamics. The constant-pH molecular dynamics algorithm used in this study is basically the same as those described in our previous studies.[26,27] Our approach consists of molecular dynamics simulations coupled with titration steps used for the evaluation of probabilities of available protonation states of the solute molecule. The probabilities are based on the electrostatic free energies of distinct protonation patterns, calculated using the Poisson−Boltzmann model for solute−solvent systems, model pK_a values of the titratable groups, and the current value of the pH.[29] The whole molecular dynamics trajectory is divided into a set of subtrajectories. These subtrajectories, generated with a standard constant temperature molecular dynamics protocol, cover a predefined period of time. The last structure from each finished subtrajectory is subject to the titration procedure. As a result of this step, at the end of each subtrajectory, the molecule can jump from its current protonation state to another one, with probability determined by the energy difference between the initial and the final state, according to a standard Monte Carlo algorithm. The protonation state of the molecule is eventually changed (by explicit proton addition or removal), and a new subtrajectory is started. The whole procedure is repeated until the constant-pH trajectory covers a desired length of time.

In the present study, we used the CHARMM[30] package for the molecular dynamics trajectory generation, and the MEAD package of Bashford[31,32] for computing the electrostatic free energy terms required for the evaluation of the pH-dependent energy levels corresponding to available protonation states of the investigated molecule.

The MD simulations used the analytical continuum solvent (ACS)[33] implemented in the CHARMM package. This mezoscopic model of solvation includes two solvent contributions to the effective energy of a solute: the electrostatic solvation free energy and the nonpolar solvation free energy. The first contribution is calculated using an analytical approximation to the solution of the Poisson equation. The second contribution is approximated by a pairwise potential that yields results similar to the surface area approximations of the hydrophobic (solvation) energy. The simulations were done at a constant temperature of 300 K, using a constant temperature/pressure algorithm based on the Berendsen method[34] with the effective solvation potential mentioned above. The solute dielectric constant was set to 1, and that of the solvent was set to 80. For the nonbonded interactions, a cutoff distance of 18 Å was used. The equations of motion were integrated using the leapfrog integrator with a time step of 0.0005 ps. The same dielectric constants, the atom descriptions, and the temperature were used in the electrostatic calculations (the finite-difference solution to the Poisson equation) with the MEAD package.

As a test of compliance of both methods used for the description of solvation effects (the analytical CHARMM potential and the finite-difference solution to the Poisson equation with MEAD), we calculated the electrostatic part of the solvation free energy for an ensemble of arbitrary chosen structures of the investigated pentapeptide, both with the MEAD and with the CHARMM package. The agreement of the results was satisfactory.

Our molecular dynamics simulations performed for the investigated peptide resulted in three sets of trajectories: two with a fixed state of Asp (charge 0 and charge −1 of the Asp side chain) and one obtained from the constant-pH simulations at pH 4. Every set consists of 20 trajectories, each starting from a different structure of the pentapeptide. The starting conformations were sampled from long MD simulations. In the case of constant-pH simulations, one-half of the starting conformations was sampled from the MD trajectory with protonated Asp, and the other half was sampled from the MD trajectory with deprotonated Asp. During each trajectory simulation, 5000 equally spaced in time structures were recorded. The length of each single fixed state trajectory is 50 ns. The length of each single constant-pH trajectory is 10.5 ns. For the constant-pH simulations, we used the time interval of 2.0 ps between successive decisions of changing the protonation state of the Asp side chain. This means that during constant-pH simulation the molecule is given opportunity to change the protonation state of the Asp2 residue every 2.0 ps, but eventual proton exchange is dependent on the current molecule's structural properties (i.e., the free electrostatic energy), the value of the pH, and a random number sampled during execution of the Metropolis Monte Carlo procedure. The value of 2.0 ps for the time interval chosen in this work seems to be suitable in the case of a well-solvated carboxylic group in a relatively small molecule like the one studied here.[18,37,38] It should be remembered that during conformational fluctuations of a polyelectrolyte molecule the pK_a values of its titratable groups can be easily significantly shifted because of the changes in their molecular environment. This can force a change in the protonation state. Proton transfer is usually very fast occurring in a sub-picosecond time range.[39,40] We also did some constant-pH simulations with the time interval of 0.25 ps. Figure 3 shows a comparison of the courses of the Asp−Lys distance during conformational transition recorded from constant-pH trajectories, with both values of the time interval, each starting from the same initial structure. It could be seen from this picture that except the amplitude of the

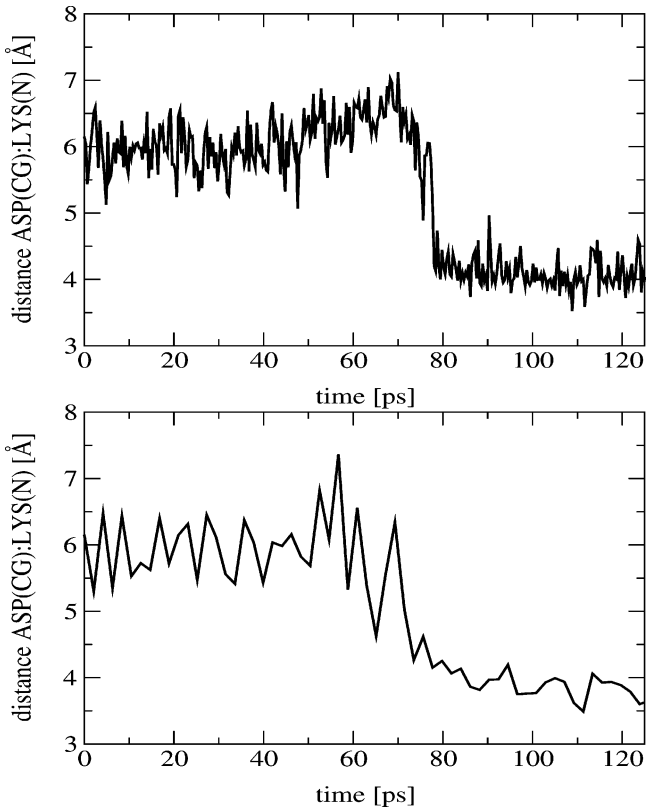

Figure 3. Course of the Asp−Lys distance from constant-pH trajectories during conformational transition. Top panel: A 0.25-ps interval between the subsequent titration steps. Bottom panel: A 2.0-ps interval between the subsequent titration steps. Both trajectories started from the same initial conditions and structure. Simulations were done at pH 4; both graphs show the raw data.

TABLE 1: Partial Charges of the Carboxylic Group of the Asp Residue in the Protonated and the Ionized State

	state of the carboxylic group		
atom	protonated (OD1)	protonated (OD2)	ionized
CB	−0.03	−0.03	−0.10
CG	0.75	0.75	0.62
OD1	−0.61	−0.55	−0.76
OD2	−0.55	−0.61	−0.76
H	0.44	0.44	

observed noise the overall behavior of the observed molecular property remains the same, no matter the time interval used.

The value of the applied time interval, discussed above, is important also due to the fact that the titration step is time-consuming and computationally demanding: The simulation of 1 ns of a constant-pH trajectory of the pentapeptide with a 2.0-ps time interval takes about 6000 s of the CPU time of a Linux workstation with a single AMD Athlon XP 3200+ processor, while the corresponding fixed protonation state simulation takes about 750 s of the CPU time.

Finally, it should be noted that we chose the generation of relatively large ensembles of trajectories each starting from a different point to address the problem of conformational sampling, because the generation of multiple trajectories can be effective for improving statistics,[41] especially in the case of a small system like the pentapeptide described in this work.

Model of Protonation States. Two states of the Asp side chain, the protonated and the ionized (with explicitly removed hydrogen ion), were modeled with the distributions of the partial charges shown in Table 1. Both oxygens of the carboxylic group of Asp (denoted OD1 and OD2 in Table 1) were considered as possible places for proton binding and were treated as separate titratable sites that cannot be occupied by a proton simultaneously. Distributions of the partial charges corresponding to the two states of the Asp side chain are derived from the CHARMM 22 force field.[35]

Titration steps of the constant-pH molecular dynamics simulation require a model pK_a of the carboxylic group of the Asp side chain, appropriate for the dielectric constants applied for description of the solute−solvent system and the sets of partial charges modeling the two states of the titratable group. We chose the blocked Asp molecule (with the N-terminus acetylated and the C-terminus amidated) as a reference compound. We collected average protonations from several constant-pH simulations of this molecule at pH 4, and using the Henderson−Hasselbalch equation

$$\mathrm{p}K_a = \mathrm{pH} - \log\left(\frac{[\mathrm{A}^-]}{[\mathrm{AH}]}\right) \tag{1}$$

we established that the model pK_a = 4 (more exactly 3.98) reproduces the expected value of 4, for the pK_a of the carboxylic group of the isolated Asp in the form defined above.

Data Denoising. Collected trajectories are of finite length, and they are burdened with a large noise. We used a running average algorithm[42] to reduce the noise in the collected data, as is shown in Figure 4.

Given a sequence of $(p)_{ii=1}^{i=N}$, a running average (or moving average) is a new sequence $(q)_{ii=1}^{i=N-n+1}$ defined from p_i by

$$q_i = \frac{1}{n}\sum_{j=i}^{i+n-1} p_i \tag{2}$$

where n denotes the length of the running average. The results presented in this work were obtained with n = 50. Usage of other values of n (between 5 and 100) gave similar results, and what is particularly important, regardless of the differences in absolute numbers regarding the investigated quantities, all of the results pointed to the same differences between constant-pH and fixed protonation state simulations.

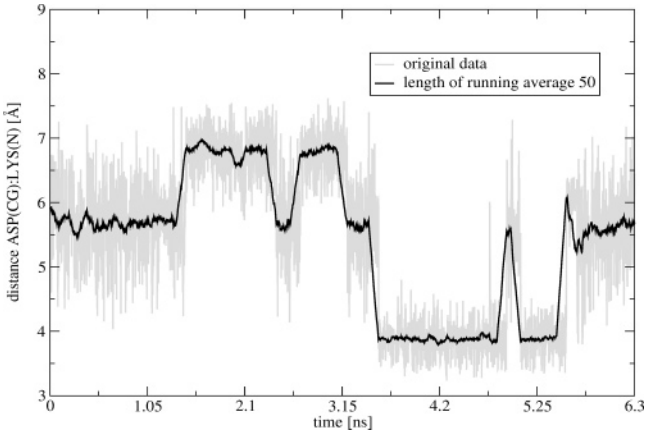

Figure 4. Example of the application of the denoising procedure to raw data.

Analysis of the Dynamic Properties. Taking the distances between the CG atom of the side chain of Asp2 and the N-atom of Lys4 (Figure 2) as a characteristic of the overall molecular structure of the pentapeptide allowed us to distinguish three general sets of states of the molecule, one with a distance of about of 4 Å and two others with greater values (as is visible in Figure 7). Then we could collect the duration times when the molecule remains in the state characterized by the shortest Asp−Lys distances. Distribution of these duration times can be analyzed in terms of an irreversible transition between two states S and L

$$\mathrm{S} \rightarrow \mathrm{L} \tag{3}$$

where state S corresponds to the shortest distance conformers and state L corresponds to all of the conformers characterized by a longer distance. (The state L is realized with at least two ensembles of conformers.) Transitions between states S and L can be considered as a Poisson process and analyzed in a way analogous to that described, for example, by Xie and Lu.[43] For this, one can replace the concentrations of the species (denoted S and L) with probabilities of finding the molecule in one of these states and write

$$\frac{\mathrm{d}P_S}{\mathrm{d}t}(t) = -kP_S(t) \tag{4}$$

where k is the rate constant for the described transition. Initial conditions for solving this differential equation are

$$P_S(t{=}0) = 1P_L(t{=}0) = 0 \tag{5}$$

and $P_S(t) + P_L(t) = 1$. The probability density, $f(\tau)$, where τ denotes time required to leave state S is

$$f(\tau) = -\frac{\mathrm{d}P_S}{\mathrm{d}t}|_{t=\tau} = k\mathrm{e}^{-k\tau} \tag{6}$$

Fitting the monoexponential curve based on eq 6 to distributions of the duration times results in the rate constant or the relaxation time of the conformational transition S → L.

Results and Discussion

Protonation Equilibria of the Asp Side Chain. Average protonations of the Asp2 residue collected from 20 constant-

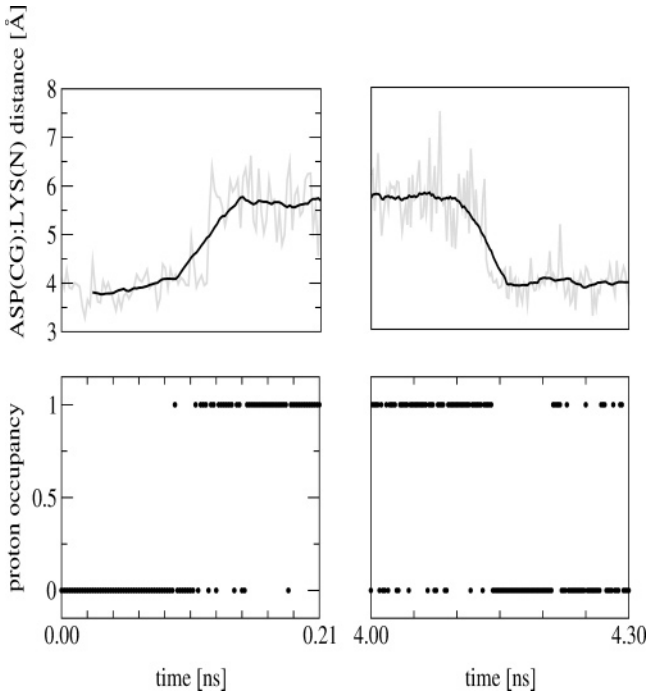

Figure 5. Examples of the evolution of the Asp−Lys distance during constant-pH molecular dynamics trajectory (top-left and top-right panels) and corresponding occupancies of the side chain of the Asp by a proton (bottom-left and bottom-right panels). The solid black line in the top panels represents denoised data. (See text for details.)

pH molecular dynamics trajectories of the acetyl-Ala-Asp-Ala-Lys-Ala-amide pentapeptide at pH 4 varied between 0.25 and 0.54, with the mean value over all 20 trajectories being 0.39 with a standard deviation of 0.07. Through the use of eq 1, the above average protonation gives the pK_a of this residue as 3.8 ± 0.1. The computed value is lower than that in the case of the blocked aspartic acid, primarily due to the interaction of Asp side chain with the positively charged Lys residue.

Figure 5 shows two short fragments of the course of the time evolution of the Asp−Lys distance registered along the molecular dynamics trajectory at constant pH, together with an indication of the protonation state of the Asp side chain assumed during subtrajectory simulations. The distances are shown both as the raw data and after denoising with 50 subsequent results used for averaging. As can be noted, short distances are accompanied by long time intervals of the deprotonated state of the Asp residue interrupted by occasional, short-lasting jumps to the protonated state. Similarly, long distances are accompanied by protonated states of Asp, but jumps to the deprotonated state for short periods of time also happen.

Analysis of the Asp−Lys Distance Distributions. Figure 6 presents the distribution of the Asp−Lys distances obtained from 5000 structures collected along one 10.5-ns constant-pH trajectory, at pH 4 (top panel), the corresponding distribution of the predicted average protonations of the side chain of Asp2 for these structures (middle panel), and the correlation between the distances and the average protonations (bottom panel).

As is visible in Figure 6, the values of the observed distance between the Asp and the Lys residues fall in the range of 3−8 Å. What also can be seen is that the conformational space of the pentapeptide can be divided into three regions distinguishable by the measured Asp−Lys distance. Important for further analysis is the state with the closest distance between those two residues. It can be clearly extracted by applying a 4.8-Å criterion

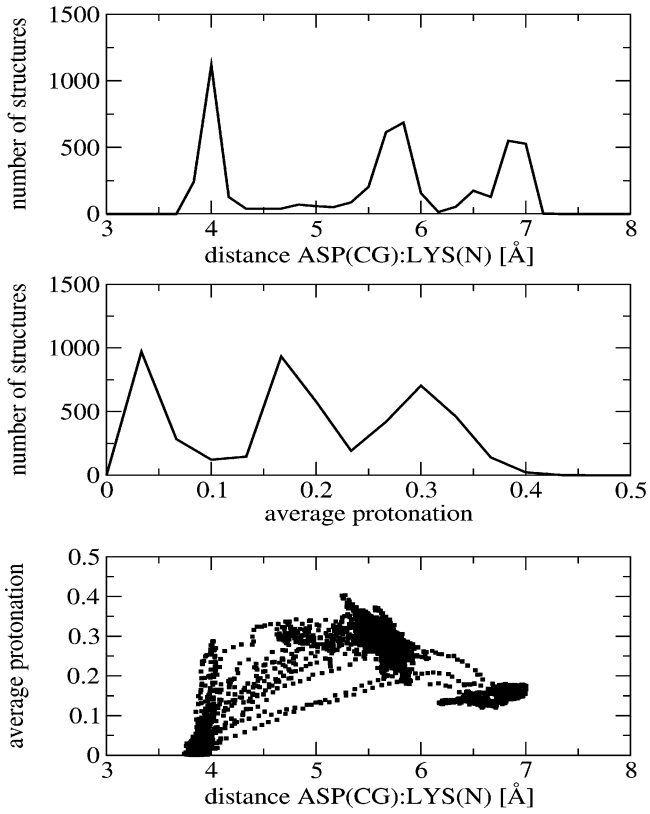

Figure 6. Distributions of the Asp−Lys distances observed in the pentapeptide acetyl-Ala-Asp-Ala-Lys-Ala-amide during a constant-pH trajectory (top panel), the average protonations of those structures (middle panel), and the correlation between the structural properties and the average protonations of the pentapeptide (bottom panel) on the basis of 5000 structures collected along a 10.5-ns constant-pH trajectory at pH 4.

to the observed distributions, giving an ensemble of structures assigned with the symbol S in eq 3.

The clustering of points in the distance−protonation correlation diagram in the bottom of Figure 6 clearly illustrates that the protonation state and the conformational properties of the pentapeptide are strongly coupled.

Asp−Lys Distance Distributions and Denoising Procedure. Figure 7 presents the Asp−Lys distance distributions obtained from all 20 simulated trajectories, 5000 structures collected from each, for the three models of the pentapeptide protonations (deprotonated Asp, top panel; protonated Asp, bottom panel; constant-pH simulation, middle panel). As can be seen, the usage of an independent starting point for each of the simulated trajectories results in the disappearance of the clear structure visible in the distance distribution shown at the top of Figure 6. This is because of the large statistical noise in the simulated data. The application of the denoising procedure to the raw data results in the reappearance of the distinguished peaks in the distance distributions.

One may also ask if the distributions characterizing constant-pH simulations can be obtained from proper averaging of the results with fixed protonation states of the titratable residues. Figure 8 shows the best (with respect to the sum of squared deviations) linear combination of the two distributions obtained from simulations with a permanently protonated and a permanently deprotonated Asp2 residue, compared with the distribution obtained from constant-pH simulations. The difference between the best linear combination and the constant-pH distribution is beyond statistical variations although relatively

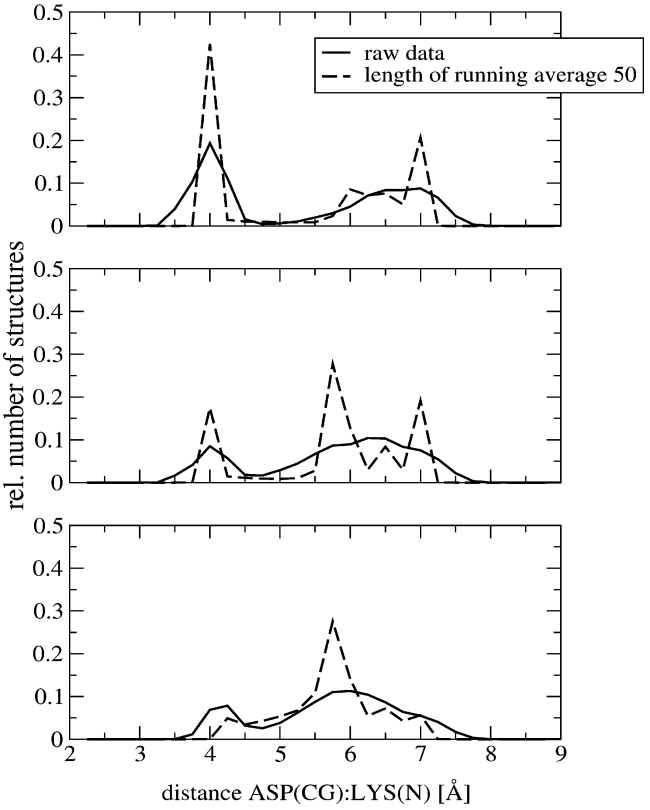

Figure 7. Distributions of the Asp−Lys distance derived from all simulated trajectories. The graphs show the distributions based on the raw data and the distributions based on the data corrected with the denosing procedure. Top panel: Pentapeptide with a permanently deprotonated Asp residue. Middle panel: Pentapeptide with the Asp residue protonable at pH 4 (constant-pH simulations). Bottom panel: Pentapeptide with a permanently protonated Asp residue.

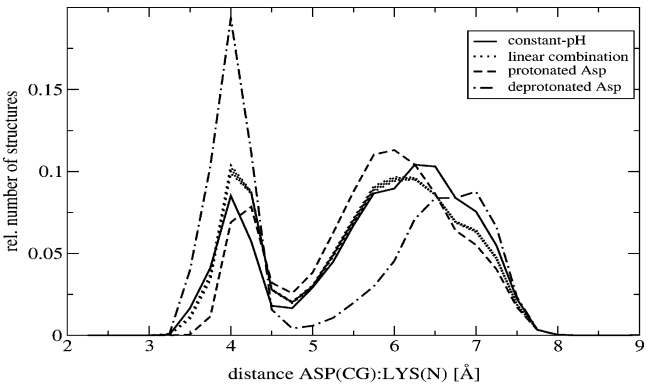

Figure 8. Attempt to reproduce the distribution of the Asp−Lys distances obtained from constant-pH simulations as a linear combination of the corresponding distributions from simulations with a fixed state of the Asp residue. The dotted line represents the linear combination of the two fixed state distributions, which is the closest to the distribution obtained from constant-pH simulations.

small. An analogous comparison made for the heptapeptide investigated in the previous study[36] exhibited significantly larger differences.

Analysis of the Dynamic Properties. As it was stated above, in the conformational space probed by the studied molecule, the three regions are distinguishable. We divided the ensemble of all of the observed structures into two groups (two distinct regions in the conformational space), one group characterized by value of the Asp−Lys distance below 4.8 Å (short-distance conformers) and the other with a value of the Asp−Lys distance above 4.8 Å (long-distance conformers), as was described above.

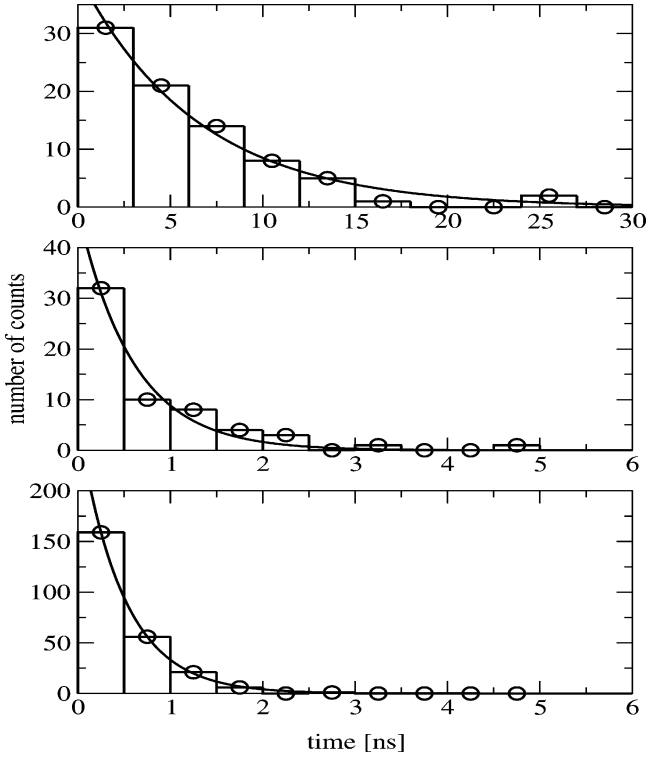

Figure 9. Distributions of the duration of the state of the acetyl-Ala-Asp-Ala-Lys-Ala-amide characterized by the closest Asp−Lys distance (histograms). Top panel: Permanently deprotonated Asp residue. Middle panel: Constant-pH simulations. Bottom panel: Permanently protonated Asp residue. Solid lines represent the monoexponential fits to the midpoints of the counts band (empty circles). For description of the fitted curves, see Table 2.

TABLE 2: Results of Fitting the Monoexponential Dependences $Nk\exp(-kt)$ to the Distribution of the Short-Distance Duration Obtained from Molecular Dynamics Simulations

protonation model of Asp	N	k (1/ns)	$1/k$ (ns)
deprotonated	260	0.16	6.44
protonated	128	2.10	0.48
protonable at pH 4	28	1.68	0.60

Distributions of the waiting times for transitions from short Asp−Lys distance conformers to those corresponding to larger distances are illustrated in Figure 9. Using a two-state formalism described above, one can study dynamic properties of the pentapeptide, such as the duration (or lifetime) of the short-distance state, by fitting monoexponential curves to the distributions obtained from molecular dynamics simulations. The fitted curves are shown in Figure 9, and the values of the resulting relaxation times and corresponding rate constants are presented in Table 2. As can be noted, the relaxation time obtained from constant-pH simulations is about 12 times shorter than that characterizing relaxations of the permanently deprotonated structure, and it is about 1.3 times longer than that characterizing relaxations of the permanently protonated structure. This seems rather surprising. The bottom panel of the Figure 6 shows that the short-distance conformers are characterized by relatively low protonation probability. Therefore, one would expect that the dynamics of transitions from short to long Asp−Lys distances should be closer to that characterizing deprotonated states. The observed picture is the opposite.

The internal motions of biomolecules cover a wide range of time scales.[44] In the review presented by Bieri and Kiefhaber,[45] one can find examples of time scales characterizing the formation of contacts and structural elements in some model systems (small peptides mainly) in the range from hundreds of picoseconds to tens of nanoseconds. The relaxation times for short to long Asp−Lys distance transitions are expected to fall in the range from tens of picoseconds to a nanosecond, which is the characteristic time scale of surface side chain rotation in proteins.[44]

Our observations can be compared with the results obtained for some other short peptides. Spörlein et al.[46] described the application of a femtosecond time-resolved spectroscopy to monitor the light-induced relaxation dynamics of a short Phe-Gly-Asp-Cys-Thr-Ala-Cys-Ala peptide, backbone-cyclized with (4-aminophenyl)azobenzoic acid, which acts as an optical trigger inducing large conformational changes in the peptide moiety. Their studies revealed sub-nanosecond conformational relaxation of the peptide. Hummer and Kevrekidis[47] presented a "coarse molecular dynamics" approach and its application to studying the kinetics of a peptide fragment dissolved in water. They determined the value of the time of interconversion between the two stable configurational basins of the "alanine dipeptide" to be about 1000 ps.

Taking into account the rather simplified model of the solute−solvent system used in this work, especially the absence of friction effects in our simulations, one cannot expect that these relaxation times are physically fully realistic. However, the short literature review, presented above, indicates that the relaxation times determined in this work are of a reasonable order of magnitude.

Because we make a comparison between two models differing in the treatment of protonation behavior of the molecules, keeping the remaining features of the two models the same, the absolute numbers for relaxation times reported in this work are less important. Our main purpose was to make an initial reconnaissance in investigations of a possible impact that solute−solvent proton exchange might have on conformational dynamics of molecules. Our study indicates that this impact can be quite serious and might be an important concern for the molecular dynamics community. It seems reasonable to expect that the differences between the results of constant-pH and fixed protonation state simulations, described in this work, will hold for more realistic models and simulation methods. Obviously, a full evaluation of the significance of the presented observations requires further studies.

Conclusions

Our work shows that the dynamic behavior of the penta-peptide acetyl-Ala-Asp-Ala-Lys-Ala-amide studied by means of traditional MD simulations differs significantly from the description given by a constant-pH MD approach. We also show that the solute−solvent proton exchange phenomena affects the average molecular properties characterizing the equilibrium distribution of the polypeptide conformations in a way that cannot be predicted by averaging results of simulations with fixed protonation states.

Acknowledgment. This work was supported by the European Union (Contract No. QLRI-CT-2002-90383) and by Warsaw University (BST-975/BF). All molecular structures were drawn with the program VMD.[48]

References and Notes

(1) Stryer, L. *Biochemistry*, 4th ed.; W. H. Freeman and Co.: New York, 1995.

(2) Pace, C. N.; Laurents, D. V.; Thomson, J. A. *Biochemistry* **1990**, *29*, 2564−2572.

(3) Pace, C. N.; Laurents, D. V.; Erickson, R. E. *Biochemistry* **1992**, *31*, 2728−2734.

(4) Yang, A.; Honig, B. *J. Mol. Biol.* **1993**, *231*, 459−474.

(5) Yang, A.; Honig, B. *J. Mol. Biol.* **1994**, *237*, 602−614.

(6) Swint-Kruse, L.; Robertson, A. D. *Biochemistry* **1996**, *35*, 171−180.

(7) Tollinger, M.; Crowhurst, K. A.; Kay, L. E.; Forman-Kay, J. D. *Proc. Natl. Acad. Sci. U.S.A.* **2003**, *100*, 4545−4550.

(8) Pletcher, C. H.; Bouhoutsos-Brown, E. F.; Bryant, R. G.; Nelsestuen, G. L. *Biochemistry* **1981**, *20*, 6149−6155.

(9) Anderson, D. E.; Becktel, W. J.; Dahlquist, F. W. *Biochemistry* **1990**, *29*, 2403−2408.

(10) Ripoll, D. R.; Vorobjev, Y. N.; Liwo, A.; Vila, J. A.; Scheraga, H. A. *J. Mol. Biol.* **1996**, *264*, 770−783.

(11) Horng, J.; Cho, J.; Raleigh, D. P. *J. Mol. Biol.* **205**, *345*, 163−173.

(12) Abbruzzetti, S.; Vlappiani, C.; Small, J. R.; Libertini, L. J.; Small, E. W. *Biophys. J.* **2000**, *79*, 2714−2731.

(13) McCammon, J. A.; Harvey, S. C. *Dynamics of Proteins and Nucleic Acids*; Cambridge University Press: Cambridge, U. K., 1987.

(14) Tuckerman, M. E.; Laasonen, K.; Sprik, M.; Parrinello, M. *J. Chem. Phys.* **1995**, *103*, 150−161.

(15) Hammes-Schiffer, S.; Tully, J. C. *J. Chem. Phys.* **1994**, *101*, 4657−4667.

(16) Bała, P.; Grochowski, P.; Lesyng, B.; McCammon, J. A. *J. Phys. Chem.* **1996**, *100*, 2535−2545.

(17) Billeter, S. R.; van Gunsteren, W. F. *J. Phys. Chem. A* **2000**, *104*, 3276−3286.

(18) Lill, M. A.; Helms, V. *J. Chem. Phys.* **2001**, *115*, 7993−8005.

(19) Baptista, A. M.; Martel, P. J.; Petersen, S. B. *Proteins: Struct., Funct., Genet.* **1997**, *27*, 523−544.

(20) Börjesson, U.; Hünenberger, P. H. *J. Chem. Phys.* **2001**, *114*, 9706−9719.

(21) Lee, M. S.; Salsbury, F. R.; Brooks, C. L. *Proteins: Struct., Funct., Bioinf.* **2004**, *56*, 738−752.

(22) Börjesson, U.; Hünenberger, P. H. *J. Phys. Chem. B* **2004**, *108*, 13551−13559.

(23) Bürgi, R.; Kollman, P. A.; van Gunsteren, W. F. *Proteins: Struct., Funct., Genet.* **2002**, *47*, 469−480.

(24) Baptista, A. M.; Teixeira, V. H.; Soares, C. M. *J. Chem. Phys.* **2002**, *117*, 4184−4200.

(25) Walczak, A. M.; Antosiewicz, J. M. *Phys. Rev. E* **2002**, *66*, 051911.

(26) Dlugosz, M.; Antosiewicz, J. M.; Robertson, A. D. *Phys. Rev. E* **2004**, *69*, 021915.

(27) Dlugosz, M.; Antosiewicz, J. M. *Chem. Phys.* **2004**, *302*, 161−170.

(28) Mongan, J.; Case, D. A.; McCammon, J. A. *J. Comput. Chem.* **2004**, *25*, 2038−2048.

(29) Antosiewicz, J.; Briggs, J. M.; Elcock, A. H.; Gilson, M. K.; McCammon, J. A. *J. Comput. Chem.* **1996**, *17*, 1633−1644.

(30) Brooks, B. R.; Bruccoleri, R. E.; Olafson, B. D.; States, D. J.; Swaminathan, S.; Karplus, M. *J. Comput. Chem.* **1983**, *4*, 187−217.

(31) Bashford, D.; Gerwert, K. *J. Mol. Biol.* **1992**, *224*, 473−486.

(32) Bashford, D. An object-oriented programming suite for electrostatic effects in biological molecules. In *Scientific Computing in Object-Oriented Parallel Environments*; Ishikawa, Y., Oldehoeft, R. R., Reynolds, J. V. W., Tholburn, M., Eds.; Lecture Notes in Computer Science 1343; Springer: Berlin, Germany, 1997, p 233.

(33) Schaefer, M.; Karplus, M. *J. Phys. Chem.* **1996**, *100*, 1578.

(34) Berendsen, H. J. C.; Postma, J. P. M.; van Gunsteren, W. F.; DiNola, A.; Haak, J. R. *J. Chem. Phys.* **1984**, *81*, 3684.

(35) MacKerell, A. D., Jr.; Bashford, D.; Bellott, R. L.; Dunbrack, R. L., Jr.; Evanseck, J. D.; Field, M. J.; Fischer, S.; Gao, J.; Guo, H.; Ha, S.; Joseph-McCarthy, D.; Kuchnir, L.; Kuczera, K.; Lau, F. T. K.; Mattos, C.; Michnick, S.; Ngo, T.; Nguyen, D. T.; Prodhom, B.; Reiher, W. E., III; Roux, B.; Schlenkrich, M.; Smith, J. C.; Stote, R.; Straub, J.; Watanabe, M.; Wiorkiewicz-Kuczera, J.; Yin, D.; Karplus, M. *J. Phys. Chem. B* **1998**, *102*, 3586−3616.

(36) Długosz, M.; Antosiewicz, J. M. *J. Phys.: Condens. Matter* **2005**, *17*, S1607−S1616.

(37) Schmidt, G. R.; Brickmann, J. *Solid State Ionics* **1996**, *77*, 3−9.

(38) Hu, -P. W.; You, -R. M.; Yen, -Y. S.; Hung, -T. F.; Chou, -H. P.; Chou, -T. P. *Chem. Phys. Lett.* **2003**, *370*, 139−146.

(39) Rini, M.; Magnes, B.-Z.; Pines, E.; Nibbering, E. T. J. *Science* **2003**, *301*, 349−352.

(40) Keiding, S. R.; Madsen, D.; Larsen, J.; Jensen, S. K.; Thøgersen, J. *Chem. Phys. Lett.* **2004**, *390*, 94−97.

(41) Auffinger, P.; Louise-May, S.; Westhof, E. *J. Am. Chem. Soc.* **1995**, *117*, 6720−6726.

(42) Kenney, J. F.; Keeping, E. S. Moving Averages. In *Mathematics of Statistics*, 3rd ed.; Van Nostrand: Princeton, NJ, 1962; Part 1, pp 221−223.

(43) Xie, X. S.; Lu, H. P. *J. Biol. Chem.* **1999**, *274*, 15967−15970.

(44) Brooks, C. L., III; Karplus, M.; Pettit, B. M. *Proteins: A Theoretical Perspective of Dynamics, Structure and Thermodynamics*; Advances in Chemical Physics 71; John Wiley and Sons: New York, 1988.

(45) Bieri, O.; Kiefhaber, T. *Biol. Chem.* **1999**, *380*, 923−929.

(46) Spörlein, S.; Carstens, H.; Satzger, H.; Renner, C.; Berrendt, R.; Moroder, L.; Tavan, P.; Zinth, W.; Wachtveitl, J. *Proc. Natl. Acad. Sci. U.S.A.* **2002**, *99*, 7998−8002.

(47) Hummer, G.; Kevrekidis, G. I. *J. Chem. Phys.* **2003**, *118*, 10762−10773.

(48) Humphreys, W.; Dalke, A.; Schulten, K. VMD−Visual molecular dynamics. *J. Mol. Graphics* **1996**, *44*, 33−38.